Magnesium Technology 2012
Edited by: Suveen N. Mathaudhu, Wim H. Sillekens, Neale R. Neelameggham, and Norbert Hort
TMS (The Minerals, Metals & Materials Society), 2012

NON-BASAL TEXTURES IN MAGNESIUM ALLOY STRIPS PRODUCED BY EXTRUSION-MACHINING

Dinakar Sagapuram[1], Mert Efe[1], Wilfredo Moscoso[3], Srinivasan Chandrasekar[2], Kevin P. Trumble[1]
Center for Materials Processing and Tribology
[1]School of Materials Engineering, [2]School of Industrial Engineering, Purdue University, West Lafayette, IN, USA
[3]Department of Electro-Mechanical and Electronics Engineering, Pontificia Universidad Catolica Madre y Maestra, Santiago, Dominican Republic

Keywords: Magnesium, Non-basal textures, Secondary slip activity, Hall-Petch effect

Abstract

A constrained chip formation technique, large strain extrusion machining (LSEM), was used to produce bulk magnesium alloy (AZ31B) strips with fine grain size (2-6 μm) and non-basal textures. These characteristics are known to enhance the final formability. The deformation temperature during extrusion-machining was varied by preheating the workpiece to a range of temperatures (50°C to 375°C). Microstructural refinement and texture evolution were studied as function of deformation temperature. It was possible to refine the grain size down to ~2 μm by restricting the dynamic grain growth at low to moderate deformation temperatures (below 320°C). LSEM was shown to be capable of resulting in non-basal textures at low deformation temperatures (below 220°C) as well as at elevated deformation temperatures (above 420°C). The influence of active deformation mechanisms and dynamic recrystallization on the texture development is also addressed.

Introduction

As the lightest structural metal, magnesium has attracted much attention due to the significant weight savings it can offer to the discrete product industry. Especially, wrought magnesium in the sheet form is highly desired for the interior automobile body frames. However, wide usage of magnesium sheet is limited by its poor room-temperature formability and high cost. The lack of formability in magnesium and its alloys is a direct result of insufficient number of active independent deformation modes required for the homogeneous deformation. Main deformation modes active at low temperatures (25-200°C) are the basal $\langle a \rangle$ slip and the $\{10\bar{1}2\}$ mechanical twinning [1]. In addition to the limited deformation modes, the plate texture (or basal texture) that develops during conventional sheet rolling also adversely affects the final formability of the sheet. The plate texture is characterized by the (0002) basal poles aligned perpendicular to the plate/sheet surface, and exhibiting fiber symmetry. The near-zero Schmid factor for the basal slip realized during the forming operations, as a result of this plate texture, results in the limited plasticity. Formability is promoted by random texture, or non-basal (or tilted basal) textures, i.e., basal poles tilted at an angle with respect to the sheet normal. However, achieving a random-textured wrought product, especially in hexagonal close packed (HCP) metals, is difficult. Non-basal textures in magnesium achieved by Mukai et al. [2] and Suwas et al. [3] through equal channel angular pressing (ECAP) were previously shown to significantly enhance the ductility/formability. However, ECAP is not suitable for direct sheet making. Besides crystallographic texture, grain size was also known to significantly influence the mechanical properties in Mg. Finer grain size was shown to enhance the strength as well as the ductility [4,5]. Here, large strain extrusion machining (LSEM) is introduced as a deformation processing technique that is capable of producing bulk magnesium strips having non-basal textures, as well as fine grain size (2-6 μm). LSEM offers control over a wide range of shear strains, strain rates, deformation temperatures, etc. In the present study, deformation temperature was varied in order to achieve a variety of textures and microstructures.

Large Strain Extrusion Machining

LSEM is a single-step deformation technique that is capable of producing metallic strip/sheet forms by employing machining and extrusion at the same time. Fig. 1 shows a schematic of the process. The set-up basically consists of a cylindrical workpiece of width, w, rotating on a spindle with a constant surface velocity (also called as deformation speed), V. A strip of final thickness, t_c, having outcoming velocity V_c is obtained by inserting the LSEM tool assembly into the workpiece at a constant feed, t, per revolution. The LSEM tool assembly, consisting of a cutting and a constraining component, results in simultaneous cutting and extrusion. For more detailed description of the process, the reader is suggested to refer Ref. [6].

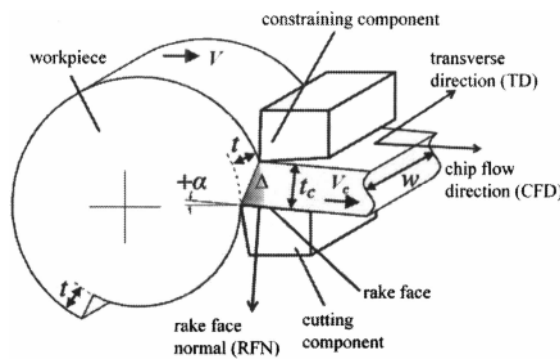

Figure 1. Schematic of LSEM.

The effective strain, $\bar{\varepsilon}$, in LSEM is given by:

$$\bar{\varepsilon} = \frac{1}{\sqrt{3}}\left[\frac{\lambda}{\cos\alpha} + \frac{1}{\lambda\cos\alpha} - 2\tan\alpha\right] \quad (1)$$

where $\lambda = t_c/t$ is the chip compression ratio and α is the rake angle. By controlling λ and α, very high effective strain (up to 3) can be imposed in a material, which helps in refining the

microstructure down to the ultrafine grain size regime [6]. The effective strain rate, $\dot{\bar{\varepsilon}}$, in LSEM is given by:

$$\dot{\bar{\varepsilon}} = \frac{\bar{\varepsilon} V}{\Delta} \tag{2}$$

where Δ is the thickness of the primary deformation zone (shaded area, Fig. 1), which was experimentally found to be quite narrow (50-150 μm thick). In LSEM, very high strain rates (up to 10^5 s^{-1}) can be obtained by adopting high $\bar{\varepsilon}$ and V. These high strain rates then cause high localized heat generation in the deformation zone. The actual deformation temperature, T_{def}, is therefore given by:

$$T_{def} = T_o + \Delta T \tag{3}$$

where T_o is the initial workpiece temperature and ΔT is the temperature rise during deformation due to high strain rate effects. Hydrostatic pressure, p, in the deformation zone is given by:

$$\frac{p}{2k} = \frac{1}{2} + 2\tan^{-1}\left(\frac{1}{2\lambda}\right) \tag{4}$$

where k is the shear strength of the material. Hydrostatic pressures as high as $1.7k$ can be achieved in LSEM. The high heat generation and hydrostatic pressure inherent in the extrusion-machining reduces the need for external heating and aids in smooth extrusion without leading to fracture.

Experimental Procedure

For extrusion-machining, a disc-shaped workpiece (6.4 mm thick) was machined from a magnesium alloy AZ31B (Mg-3 wt.% Al-1 wt.% Zn) tooling plate, supplied by ThyssenKrupp Materials NA, Inc. It should be noted that the thickness of the workpiece, w, corresponds to the final strip width. A constant rake angle, α, of 5° was used. The chip compression ratio, λ, was fixed at ~0.75 by choosing t = 0.25 mm and t_c = 0.19 mm. According to Eq. 1, effective strain, $\bar{\varepsilon}$, was therefore kept constant at 1.1. A constant deformation speed, V, of 0.5 m/s was used. Strain rate, $\dot{\bar{\varepsilon}}$, was therefore fixed at 0.55×10^4 s^{-1}, according to Eq. 2. Deformation temperature, T_{def}, was varied by controlling the initial workpiece temperature (or preheating temperature), T_o. The temperature rise, ΔT of 170°C was estimated from the cutting forces measured using a piezoelectric dynamometer. Details of the heat-partition model used for calculating the temperature rise can be found elsewhere [7]. The preheating temperature was found to have a negligible effect on ΔT. Assuming that the heat-partition model is valid even at higher temperatures, T_{def} can be given by: T_{def} (°C) = T_o (°C) + 170°C. A range of preheating temperatures from 50 to 375°C were used. This accordingly corresponds to a variation of T_{def} from 220 to 545°C.

For optical microscopy, chip flow direction (CFD)-rake face normal (RFN) plane (refer to Fig. 1) of the samples was polished according to standard metallographic procedures and etched with a picric acid solution (100 ml ethanol, 10 ml water, 6 g picric acid, and 5 ml acetic acid). Average grain size was estimated using the linear intercept method. Hardness measurements were carried out on the CFD-RFN plane. For crystallographic texture analysis, an X-ray area detector diffraction system (GADDS, Bruker AXS) was used. A Rietveld refinement program, MAUD [8], was used to analyze the diffraction data and construct the pole figures.

Results

The as-received AZ31B tooling plate exhibited a plate texture (i.e., in-plane basal fiber texture) and an equiaxed microstructure (images not shown here). The grain size was 16 ± 2 μm and the hardness was 58 HV. The effect of T_o on the microstructure development in the LSEM strips is given in Fig. 2. All the strips exhibited equiaxed microstructures. Fig. 3 shows the effect of T_o

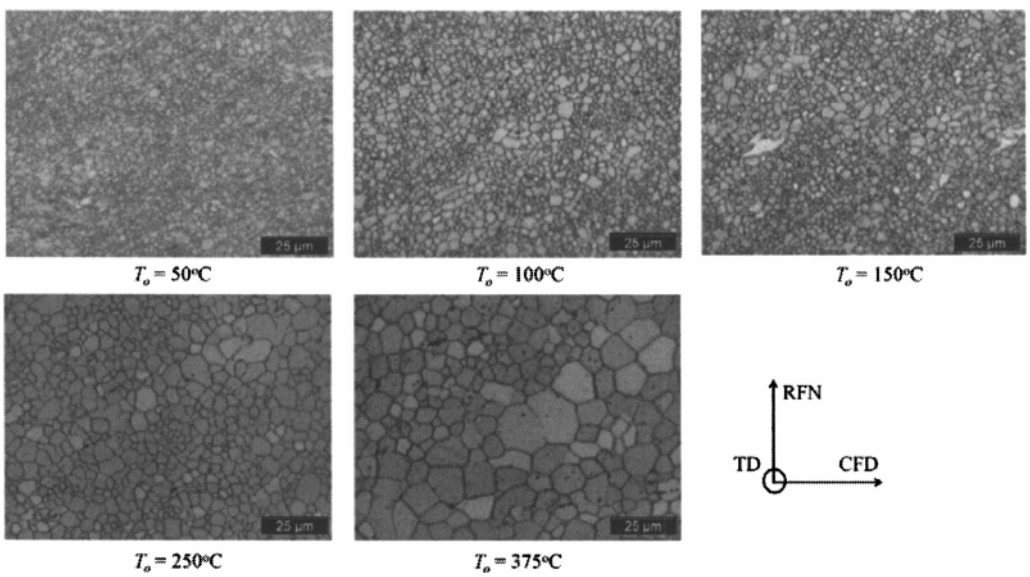

Figure 2. Microstructure development in the LSEM strips as a function of workpiece preheating temperature, T_o. (TD: transverse direction).

on the final grain size, d. Standard deviations are given by the error bars. It can be seen that d remains almost constant initially and increases rapidly when T_o is greater than 150°C. Increase in T_o from 50 to 375°C lead to a corresponding increase in d from 1.7 to 6.4 μm. It is noteworthy that extrusion-machining is capable of refining the microstructure by 2-10 times in a single step, as opposed to the standard multi-step deformation techniques.

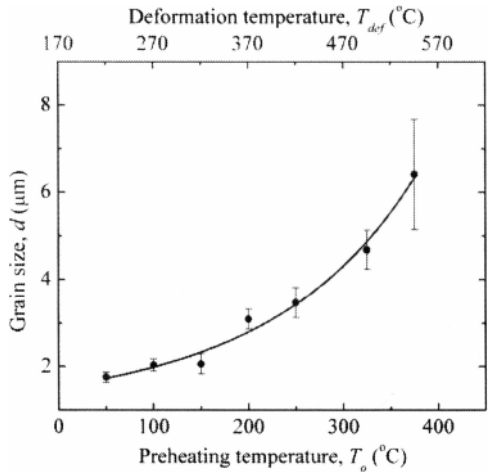

Figure 3. Variation of d as a function of T_o.

The Hall-Petch relationship [9] is typically exhibited by metals and alloys when grain size is in the microcrystalline range. It is given by:

$$H = H_o + K_H d^{-1/2} \quad (5)$$

where H_o and K_H are called the Hall-Petch constants. In order to examine the Hall-Petch relationship in the AZ31B strips produced

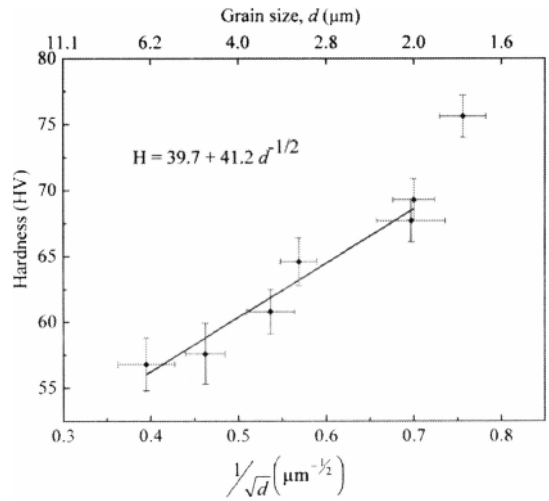

Figure 4. Hall-Petch plot for AZ31B.

by LSEM, hardness is plotted against $d^{-1/2}$ in Fig. 4. The AZ31B strips obeyed the Hall-Petch relationship with H_o = 39.7 and K_H = 41.2.

Evolution of texture with T_o is shown in Fig. 5. The (0002) and $(10\bar{1}0)$ pole figures were measured from the TD-CFD plane (refer to Fig. 1). A mirror symmetry about the CFD axis in the pole figures can be observed. Texture intensity is given in the unit, multiples of a random distribution (mrd). When T_o is low (50°C), extrusion-machining was found to result in two distinct texture components having a similar intensity: a tilted basal texture component, and a basal texture component. The tilted basal texture component is characterized by (0002) basal poles tilted at an angle of ~30° away from RFN toward CFD, while the basal texture component has basal poles aligned parallel to RFN.

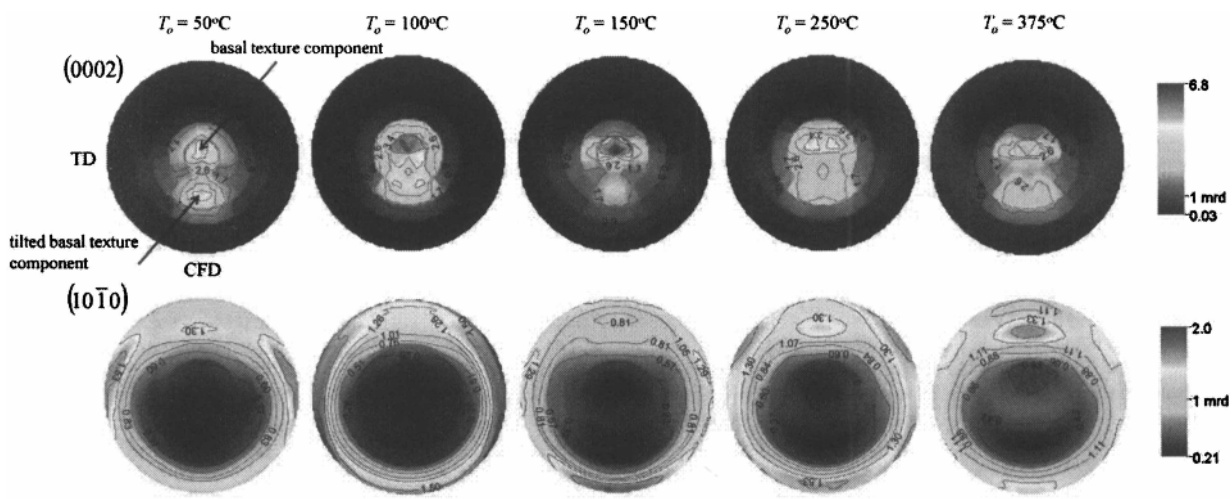

Figure 5. Texture evolution in the LSEM strips with increasing T_o.

From the $(10\bar{1}0)$ pole figures, it seems that both the tilted basal and basal texture components exhibit $< 0001 >$ fiber symmetry. With increasing T_o, intensity of the tilted basal texture was found to gradually decrease, while that of the basal texture component increased, and reached a maximum value of 6.8 mrd at T_o = 150°C. Correspondingly, the basal texture component no longer exhibits $< 0001 >$ fiber symmetry. Instead, $(10\bar{1}0)$ poles are aligned parallel to CFD. Further increase in T_o to 250°C resulted in a decrease in texture intensity and splitting of the basal poles about RFN by ± 10-20° along TD. The corresponding $(10\bar{1}0)$ pole figure indicates that the basal poles have regained the fiber symmetry. With further increase in T_o to 375°C, no qualitative changes in the texture were observed. It is interesting to note that, with increasing T_o, the peak intensity value initially increased from 5 mrd at T_o = 50°C, reached a maximum of 6.8 mrd at T_o = 150°C, and then started decreasing, where it finally dropped down to 4 mrd at T_o = 375°C.

Discussion

The fine equiaxed grain structures (Fig. 2) found in the LSEM strips and the grain size variation with deformation temperature (Fig. 3) can be explained by dynamic recrystallization (DRX) followed by dynamic grain growth. Grain size refinement from 16 μm in the as-received material to 1.7 μm in the strip processed at a low temperature of T_o = 50°C is a result of high shear strain in extrusion-machining and restricted grain growth due to warm deformation temperature (T_{def} = 220°C). Grain size remained almost constant up to T_o = 150°C. However, when T_o is greater than 150°C, grain size started to increase rapidly. This suggests the increased activity of dynamic grain growth at moderate temperatures (T_{def} > 320°C ≈ 0.5T_m).

The Hall-Petch effect in AZ31B (Fig. 4) confirms the grain size strengthening widely known in metals. The values of the Hall-Petch constants found in this study (H_o = 39.7, K_H = 41.2) are in fair agreement with the literature, where values of H_o = 40-47 and K_H = 42-50 were reported for the extruded and ECAP'ed AZ31 [10]. It should be noted that the LSEM strips, although having quite different textures (Fig. 5) from one another, still exhibit the Hall-Petch effect. This, indeed, is peculiar since texture is known to have a significant influence on the strength in magnesium alloys.

Deformation texture evolution in a material is primarily influenced by the stress state of deformation, active slip systems, and thermally activated processes like DRX. It is believed that the two texture components observed in the low temperature strip (T_o = 50°C) is a result of extensive basal slip in the primary and secondary deformation zones. The secondary deformation zone arises from the friction between the rake face and the outcoming strip [11], especially under conditions where λ is less than 1. The shear in the primary deformation zone due to the basal slip aligns the basal planes nearly parallel to the shear plane, resulting in the tilted basal texture component. Similarly, the basal texture component occurs due to the shear in the secondary deformation zone, which results in alignment of the basal planes parallel to the rake face. Formation of the basal texture component is typical in rolling/compression type deformation, while the tilted basal texture component is observed in shear-based deformation as in ECAP [3,12]. The increase in T_o to 100°C lead to the strengthening of basal texture component, accompanied by a decrease of tilted basal texture component intensity. This type of textural change with increasing T_{def} in extrusion-machining was previously found to coincide with the beginning of discontinuous dynamic recrystallization (DDRX) [13]. DDRX is a type of DRX, where new grains nucleate near the original grain boundaries, having orientations different from the orientations of deformed grains. The beginning of DDRX was also found to be accompanied by a sharp hardness drop, which seems to be true even in the present study. In Fig. 4, a sharp hardness drop occurs when grain size is increased from 1.7 μm to 2 μm. Hence, the change in texture with increasing T_o from 50 to 100°C is believed to be due to DDRX. However, the reason why DDRX seems to be strengthening particularly the basal texture component is currently unknown, and needs further investigation. With increasing T_o to 150°C, basal texture is further intensified and displays a maximum peak intensity of 6.8 mrd, presumably due to the increased DDRX as a result of higher T_{def}. The reason for the alignment of $(10\bar{1}0)$ poles with CFD for this condition is not clear. Further increase in T_o to 250°C caused splitting of basal poles away from RFN along TD, which is surprising in AZ31B. This kind of basal pole splitting in TD is usually a characteristic of rolling textures of HCP metals like Zr [14], where prismatic $\langle a \rangle$ slip is dominant. ECAP of Mg-4 wt.% Li, which is known to increase prismatic slip activity, was also shown to result in a texture component tilted towards the flow plane normal direction [12]. Since the extrusion-machining geometry can be compared to that of ECAP, it is presumed that increased secondary slip activity (i.e., prismatic $\langle a \rangle$ slip or pyramidal $\langle c + a \rangle$ slip, or both) at elevated temperatures (T_o > 250°C, T_{def} > 420°C) as the reason for the basal pole splitting in TD. The drastic decrease in critical resolved shear stress (CRSS) for secondary slip systems with temperature [15] is also in agreement with this assumption. Further increase in T_o to 375°C lead to no significant changes in texture, except for the decreased peak intensity value. The texture weakening at elevated deformation temperatures is, at present, not clear.

Conclusions

LSEM was shown to be capable of achieving a variety of non-basal textures in fine grained AZ31B strips. This ability of LSEM to control the texture, as well as refine the microstructure, will be very useful in designing the final mechanical properties like strength and formability. Deformation temperature was found to greatly influence the microstructure and texture evolution. Dynamic grain growth was found to be restricted at low to moderate deformation temperatures (≤ 320°C), resulting in fine grain sizes (~2 μm). At elevated deformation temperatures, grain size increased (3-6 μm) due to dynamic grain growth. AZ31B strips were also shown to exhibit the Hall-Petch relationship independent of the texture. Low temperature basal slip resulted in a texture having two components: a tilted basal and a basal texture component. Thermally activated DDRX at moderate temperatures (270-320°C) was found to strengthen the basal texture and weaken the tilted basal texture. At elevated temperatures (≥ 420°C), basal pole splitting in the strip transverse direction was observed. Increased activity of secondary slip systems with temperature is presumed to be the cause for this basal pole splitting. Further increase in temperature seems to weaken the texture without changing the texture character. Finally, formability enhancement

in AZ31B as a result of the LSEM non-basal textures (i.e., textures containing the tilted basal texture component or exhibiting the basal pole splitting) and fine grain size looks promising.

Acknowledgements

Support through NSF-CMMI-MPM-0800481 and DOE PNNL-DE-AC06-76RL01830 is gratefully acknowledged.

References

1. I.J. Polmear, "Magnesium Alloys and Applications", *Materials Science and Technology*, 10 (1994), 1-16.

2. T. Mukai, M. Yamanoi, H. Watanabe, and K Higashi, "Ductility Enhancement in AZ31 Magnesium Alloy by Controlling its Grain Structure", *Scripta Materialia*, 45 (2001), 89-94.

3. Satyam Suwas, G. Gottstein, and R. Kumar, "Evolution of Crystallographic Texture during Equal Channel Angular Extrusion (ECAE) and its Effects on Secondary Processing of Magnesium", *Materials Science and Engineering A*, 471 (2007), 1-14.

4. Edward F. Emley, *Principles of Magnesium Technology* (Oxford, New York, Pergamon Press, 1966).

5. L. Jin, D. Lin, D. Mao, X. Zeng, and W. Ding, "Mechanical Properties and Microstructure of AZ31 Mg Alloy Processed by Two-step Equal Angular Channel Extrusion", *Materials Letters*, 59 (2005), 2267-2270.

6. W. Moscoso, M.R. Shankar, J.B. Mann, W.D. Compton, S. Chandrasekar, "Bulk Nanostructured Materials by Large Strain Extrusion Machining", *Journal of Materials Research*, 22 (2007), 201-205.

7. J.H. Wiener, "Shear-plane Temperature Distribution in Orthogonal Cutting", *Transactions of the American Society of Mechanical Engineers*, 77 (1955), 1331-1341.

8. L. Lutterotti, M. Bortolotti, G. Ischia, I. Lonardelli, and H.R. Wenk, "Rietveld Texture analysis from Diffraction Images", *Zeitschrift für Kristallographie Supplements*, 26 (2007), 125-130.

9. E.O. Hall, "The Deformation and Ageing of Mild Steel: II Characteristics of Lüders Bands", *Proceedings of the Physical Society B*, 64 (1951), 742-747.

10. W.J. Kim, Y.K. Sa, "Micro-extrusion of ECAP Processed Magnesium Alloy for Production of High Strength Magnesium Micro-gears", *Scripta Materialia*, 54 (2006) 1391-1395.

11. M. Sevier, H.T.Y. Yang, W. Moscoso, and S. Chandrasekar, "Analysis of Severe Plastic Deformation by Large Strain Extrusion Machining", *Metallurgical and Materials Transactions A*, 39A (2008), 2645-2655.

12. S.R. Agnew, P. Mehrotra, T.M. Lillo, G.M. Stoica, and P.K. Liaw, "Texture Evolution of Five Wrought Magnesium Alloys during Route A Equal Channel Angular Extrusion: Experiments and Simulations", *Acta Materialia*, 53 (2005), 3135-3146.

13. D. Sagapuram, M. Efe, W. Moscoso, S. Chandrasekar, and K.P. Trumble, "Deformation Temperature Effects on Microstructure and Texture Evolution in High Strain Rate Extrusion-Machining of Mg-AZ31B", *Proceedings of the 16th International Conference on Texture of Materials*, Bombay, India, Dec, 2011.

14. Y.N. Wang, and J.C. Huang, "Texture Analysis in Hexagonal Materials", *Materials Chemistry and Physics*, 81 (2003), 11-26.

15. S.E. Ion, F.J. Humphreys, and S.H. White, "Dynamic Recrystallization and Development of Microstructure during the High Temperature Deformation of Magnesium", *Acta Metallurgica*, 30 (1982), 1909-1919.